Using Proton Irradiation to Probe the Origins of Low-frequency Noise Variations in SiGe HBTs

Zhenrong Jin[1], Jarle A. Johansen[1,2], John D. Cressler[1],
Robert A. Reed[3], Paul W. Marshall[4], and Alvin J. Joseph[5]

[1] School of Electrical and Computer Engineering,
Georgia Institute of Technology, Atlanta, GA 30332, USA
[2] Institute of Physics, University of Tromsø, NORWAY
[3] NASA GSFC, Greenbelt, MD 20771, USA
[4] a consultant to NASA GSFC, Greenbelt, MD 20771, USA
[5] IBM Microelectronics, Essex Junction, VT 05452, USA

35-Word Abstract

Proton irradiation is used to probe the physical origins of low-frequency noise variation in SiGe HBTs. After irradiation the noise level degradation is negligible, but the noise variation decreases and depends on geometry and bias.

Author Contact Information:

Zhenrong Jin
School of Electrical and Computer Engineering, 791 Atlantic Drive, N.W.
Georgia Institute of Technology, Atlanta, GA 30332-0250, USA

Tel: (404) 385-4307 / Fax: (404) 894-4641 / e-mail: zhenrong@ece.gatech.edu

Suggested Session:
"Devices and Integrated Circuits"

Oral Presentation Preferred

Using Proton Irradiation to Probe the Origins of Low-frequency Noise Variations in SiGe HBTs

Zhenrong Jin, Jarle A. Johansen, John D. Cressler,
Robert A. Reed, Paul W. Marshall, and Alvin J. Joseph

ABSTRACT—We use proton irradiation to probe the origins of the geometry-dependent variation of low-frequency noise in 120 GHz SiGe HBTs for the first time. Before irradiation, small-sized transistors show a strong variation in noise magnitude across many samples, whereas the noise in larger devices is more statistically reproducible. Although the noise magnitude shows little degradation after $2 \times 10^{13} p/cm^2$ irradiation, the observed noise variation decreases. Its dependence on both geometry and bias is quantified. This fundamental geometrical scaling effect is investigated using theoretical calculations based on the superposition of G/R noise sources.

I. Introduction

SiGe HBT BiCMOS technology offers high-level integration, low cost, and high-speed, and is being increasingly used for mixed-signal circuit applications. Low-frequency noise (LFN) in transistors usually has a $1/f$-like spectrum, and sets the lower limit on the detectable signal level, not only in the low frequency range, but also at high frequencies via the up-conversion to the carrier frequency through the non-linearities of the device (phase noise). Understanding LFN is thus a crucial design issue in direct-conversion receivers, oscillators, synthesizers, amplifiers, and mixers for digital, analog and optoelectronics applications.

Transistors are aggressively scaled (downsized) in order to improve performance and integration level. One design issue associated with geometrical scaling is that the LFN often shows a different frequency dependence for each individual device [1], [2], and this can directly affect both circuit performance and accurate modeling. This LFN variation has been observed in BJTs and SiGe HBTs in very small-sized devices [1], [2], and the fundamental noise mechanism is regarded as the superposition of individual trapping/detrapping processes due to the presence of G/R centers in the device. Each G/R center contributes a Lorentzian-type ($1/f^2$) noise signature. Given a sufficient number of traps and a particular distribution of characteristic time constants associated with the G/R centers, these Lorentzian processes combine to produce the observed $1/f$ noise behavior [3]. At sufficiently small size, however, the total number of traps is small enough that non-$1/f$ behavior, and large statistical variations, can be observed. These trapping/detrapping processes modulate the number of carriers, and thus are best described by number fluctuation theory [1]-[12] instead of mobility fluctuation theory [13]-[17].

In this work, we intentionally introduce additional traps into the transistor via proton irradiation in order to probe the physical origins of the observed LFN variations in 120 GHz SiGe HBTs. In addition, this work provides valuable information on whether such LFN variations are potentially important in space-borne communications applications.

This work was supported by DTRA under the Radiation Tolerant Microelectronics Program, NASA-GSFC under the Electronics Radiation Characterization Program, a Fulbright Fellowship (J.A. Johansen), On Semiconductor, SRC under Task 1022, Yamacraw at Georgia Tech, and an IBM University Partner Award.
Z. Jin and J. D. Cressler are with School of Electrical and Computer Engineering, Georgia Institute of Technology, Atlanta, GA 30332, USA. Tel: (404) 385-4307 / Fax: (404) 894-4641 / E-mail: zhenrong@ece.gatech.edu.
J. A. Johansen is with Institute of Physics, University of Tromsø, 9037 Tromsø, NORWAY.
A. J. Joseph is with IBM Microelectronics, Essex Junction, VT 05452, USA
R. A. Reed is with NASA GSFC, Greenbelt, MD 20771, USA.
P. W. Marshall is a consultant to NASA GSFC, Greenbelt, MD 20771, USA.

II. Experiment

The transistors are from a fully-integrated commercial $0.20\mu m$ 120 GHz peak f_T SiGe technology [18]. Since the dominant noise source in the common-emitter configuration is associated with the base current, the base current noise spectrum S_{I_B}, was investigated [1], [2], [6], and [7]. The transistor was biased in a common-emitter configuration with $V_{CB} = 0V$. The details of the noise measurement system can be found in [19]. Transistors with emitter areas of $A_E = 0.82 \times 3.22\mu m^2$, $0.30 \times 1.86\mu m^2$ and $0.22 \times 0.66\mu m^2$ were measured, and are hereafter referred to as "large", "medium", and "small" devices. For meaningful statistical comparisons, six transistors of each transistor size were characterized on separate die from the same wafer.

The samples were diced and attached to a ceramic holder and directly exposed with terminals floating to $62.5 MeV$ protons at the Crocker Nuclear Laboratory cyclotron located at the University of California at Davis. A total accumulated fluence of 2×10^{13}p/cm^2 was used. Dosimetry measurements used a 5-foil secondary emission monitor calibrated against a Faraday cup. Ta scattering foils located several meters upstream of the target establish a beam spatial uniformity of 15% over a 2 cm radius circular area. Beam currents from about 5 pA to 50 nA allow testing with proton fluxes from 10^6 to 10^{11} protons/cm^2/sec. The dosimetry system has been previously described in [20], [21], and is accurate to about 10%.

III. Measurement Results

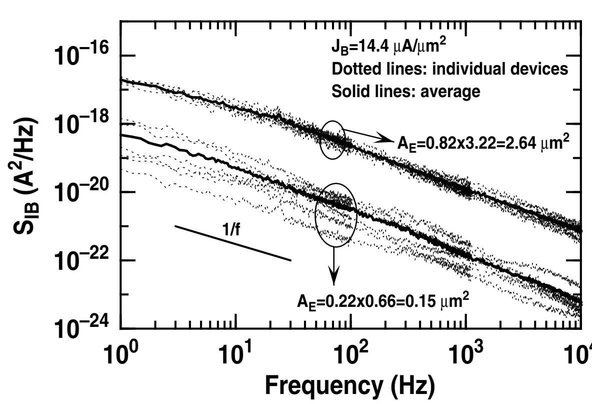

Fig. 1. Noise spectra from small and large transistors at J_B=14.4μm^2. Six samples of each size are shown.

In Fig. 1, we compare the measured noise spectra from six samples of small and large SiGe HBTs. The devices were biased at the same base current density to obtain a similar forward voltage bias on the base-emitter junction. The dashed lines in the figure represent the noise spectra from the individual devices, while the solid lines are the averaged spectra across all devices. We observe a large statistical variation of the LFN spectra between different samples of the small transistors, whereas the large devices show a very similar LFN signature among different samples, consistent with our earlier results on a 90 GHz SiGe technology [2]. The large transistors individually exhibit a $1/f$ dependence, and hence the average over all devices shows the same frequency dependence. More interestingly, however, the small devices, which individually show a strongly variable frequency dependence, also average to a straight-line $1/f$ LFN spectrum across this frequency range. The variation in noise between the samples of the same geometry was quantified using a variation coefficient, δ, given by the standard deviation formula [1], [2]:

$$\delta = \frac{1}{S_{I_{B,avg}}}\sqrt{\frac{1}{N-1}\sum_{i=1}^{N}\left(S_{I_{B,i}} - S_{I_{B,avg}}\right)^2} \qquad (1)$$

$$S_{I_{B,avg}} = \frac{1}{N}\sum_{i=1}^{N} S_{I_{B,i}}$$

where i indicates the $i'th$ sample, and N is the total number of samples. The noise variation dependence on base current density

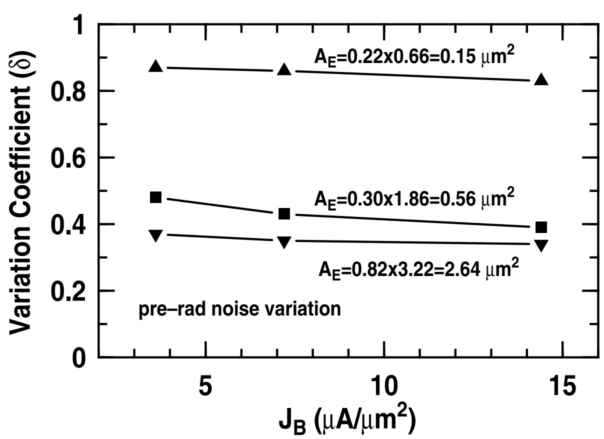

Fig. 2. Noise variation for measured noise spectra versus J_B before irradiation.

is shown in Fig. 2. The observed noise variation is not strongly dependent on base current density. This is consistent with our observation of the measured noise spectra, which only increase in magnitude, and not in shape with increasing bias current.

Interestingly, after irradiation, the average noise magnitude shows little degradation at the three bias current densities for the three geometries as shown in Fig. 3. However, as shown in Fig. 4, the noise variation shows a significant decrease for the small devices, especially at low J_B, but shows a smaller decrease for the medium and large devices. The noise variation thus now depends both on geometry and bias. It is clear that radiation changes the noise variation in these SiGe HBTs.

The noise was measured with the base current held constant from sample-to-sample. Due to small variations in the dc parameters, we observed slight variations in the base-emitter voltage needed to obtain the desired base current, and also a variation in the resulting collector current due to variations in the current gain across the wafer. The observed variation in current gain and V_{BE} was also calculated using the standard deviation formula. The results are shown in Fig. 5. The variation in the dc parameters is negligible compared to the large variation in the noise, and hence the observed noise variation is clearly not caused by variations in the transistor dc parameters alone.

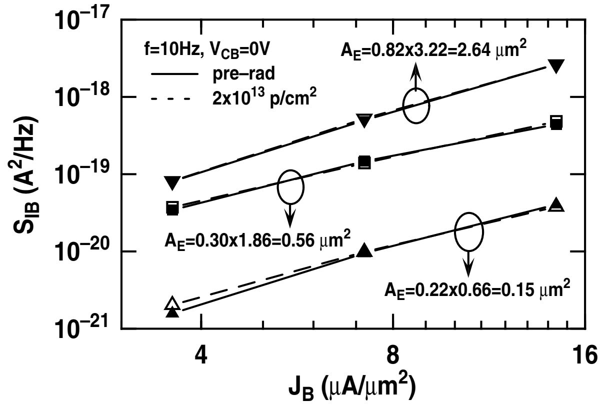

Fig. 3. Noise magnitude versus J_B at 10 Hz before and after irradiation.

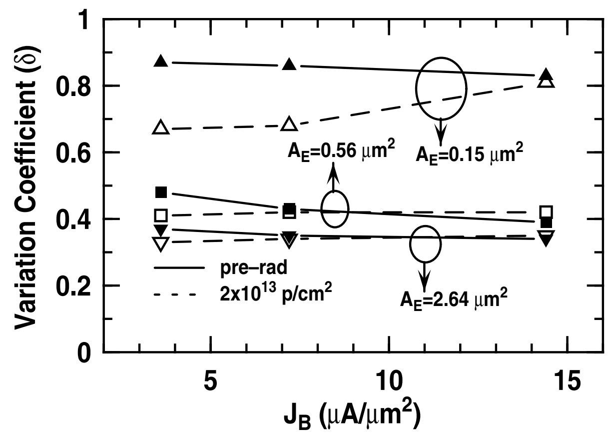

Fig. 4. Noise variation for measured noise spectra versus J_B before and after irradiation.

IV. Model and Discussion

A. Pre-radiation

An intuitive explanation for the physical basis of carrier number fluctuations in BJTs centers on the trapping/detrapping of carriers by traps at the interfaces or oxide layers [9]. The noise of each individual trapping/detrapping process theoretically exhibits a Lorentzian spectrum $(1/f^2)$ which can be expressed as

$$S_{I_B} = \alpha\frac{\tau}{1+(2\pi f\tau)^2} \qquad (2)$$

where α is the amplitude (with units of A^2), and τ is the characteristic time constant. The noise spectrum is flat at low frequency and decreases as $1/f^2$ at high frequency. The superposition of a large number of Lorentzian spectra with $1/\tau$ distribution results in the usually observed $1/f$ spectrum [3], as illustrated in Fig. 6.

In [2], the $1/f$ noise in SiGe BJTs was expressed as the superposition of such Lorentzian noise sources. Following the same

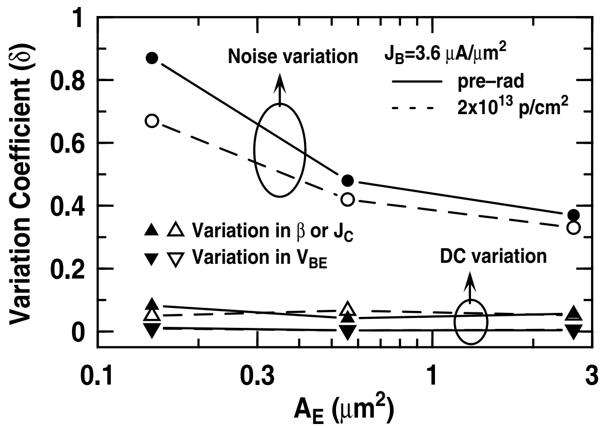

Fig. 5. Noise and *dc* parameter variations from measured data versus A_E before and after irradiation.

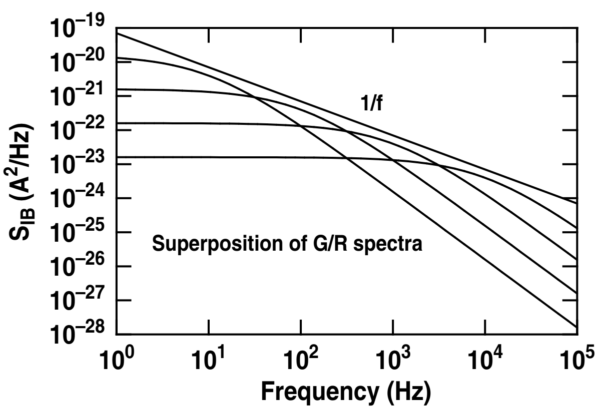

Fig. 6. Superposition of Lorentzian (G/R) spectra yields a 1/f spectrum.

procedure, to obtain a best fit to the pre-radiation measurement data, an empirical expression of the low-frequency noise spectrum can be written as [1], [2]:

$$S_{I_B} = \sum_{i}^{N_T} A \frac{A_E^{0.2} J_B^{2.4} \tau_i}{1 + (2\pi f \tau_i)^2} \tag{3}$$

where A is a constant, τ_i is the characteristic time constant of the i^{th} independent trap and has to be distributed as $1/\tau$ to produce a $1/f$ spectrum, and N_T is the total number of traps in the device and proportional to A_E. When N_T is large enough, which is the case in the large device, (3) yields a $1/f$ spectrum. When N_T is small enough, corresponding to the small device case, the spectrum modeled by this equation will show a deviation from $1/f$ behavior. Five hundred different characteristic time constants were generated over the range $1/(2\pi \times 10^7)$ to $1/(2\pi \times 10^{-3})$ with a $1/\tau$ distribution. To best fit the data, three was chosen as the trap number in the small device, twelve was chosen as the trap number in medium device, and fifty was chosen as the trap number in large device. Characteristic time constants associated with each trap were randomly drawn for every calculation of the small, medium and large devices (A=$1.1\times10^{-26} cm^{4.4}/A^{0.4}$).

Six individual calculations (to mimic the six independent measurements) were performed for each size device, and the noise variation coefficient of the six calculated spectra is shown in Fig. 7, consistent with the measured data. The calculated noise variation is bias independent as expected from (1) and (3). These calculations confirm that a small number of traps indeed leads to the observed large noise variation in the small devices.

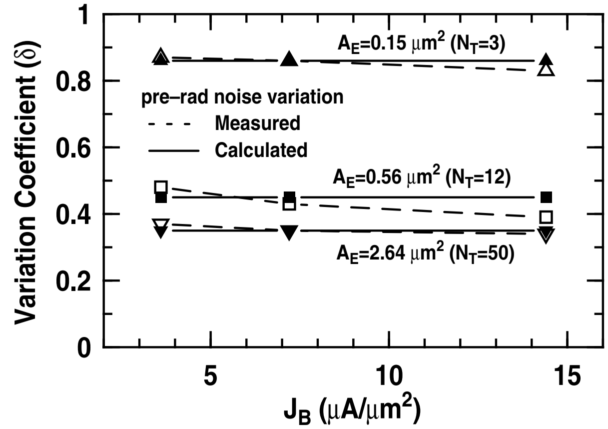

Fig. 7. Noise variation from measured and calculated noise spectra versus J_B before irradiation. The number of traps used in the calculations is indicated for each size.

B. Post-radiation

Proton irradiation generates traps around device emitter perimeter in these SiGe HBTs [19]. These traps create a non-ideal base current component due to increased space-charge region(SCR) G/R center recombination current near the surface, as confirmed in Fig. 8.

Assuming the radiation-induced noise increase is mainly due to these peripheral traps, the radiation-induced LFN increase $S_{I_{B,SCR}}$ can be expressed as [19] :

$$S_{I_{B,SCR}} = C J_B n_{T,R} P_E \frac{\alpha_H}{f} \tag{4}$$

where C is a constant that is independent of bias and geometry, and $n_{T,R}$ is the peripheral trap density induced by radiation. Thus, radiation-induced $S_{I_{B,SCR}}$ shows an J_B and P_E dependence. By analogy to the pre-radiation behavior, assuming each radiation-induced trap has a Lorentzian spectrum, the radiation-induced noise power spectral density $S_{I_{B,SCR}}$ can also be expressed as a superposition of Lorentzian spectra provided that the superposition shows a J_B and P_E dependence when the number of traps is large enough, as expected from (4). Hence, an empirical expression for $S_{I_{B,SCR}}$ can be obtained as:

$$S_{I_{B,SCR}} = \sum_{j=1}^{n_{T,R}} B \frac{J_B \tau_j}{1 + (2\pi f \tau_j)^2} \tag{5}$$

where τ_j is the characteristic time constant associated with the j^{th} radiation-induced trap, B is a constant, and $n_{T,R}$ is the trap number induced by radiation, which is proportional to the emitter perimeter.

The post-radiation spectrum can be obtained by adding (3) and (4):

$$S_{I_B,S} = S_{I_B} + S_{I_{B,SCR}} \tag{6}$$

$$= \sum_{i=1}^{N_T} A \frac{J_B^{2.4} A_E^{0.2} \tau_i}{1 + (2\pi f \tau_i)^2} + \sum_{j=1}^{n_{T,R}} B \frac{J_B \tau_j}{1 + (2\pi f \tau_j)^2} \tag{7}$$

Since S_{I_B} increases much faster than $S_{I_{B,SCR}}$ when J_B increases, S_{I_B} can be the dominant term at high bias in (7). It is thus possible to see that the noise variation shows a decrease at low J_B, rather than at high J_B for same-sized devices, as shown in Fig. 4. At a fixed J_B, since the small number of pre-radiation traps and the large variation in the small device, a few more radiation-induced traps can effectively decrease this noise variation. It is thus possible to see a relatively large decrease of noise variation for small devices compared to the medium and large devices.

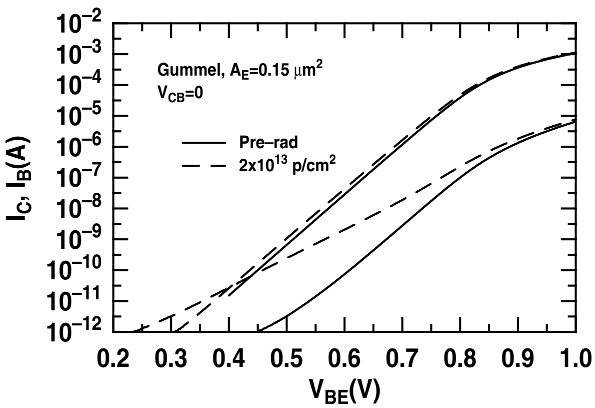

Fig. 8. I_C and I_B versus V_{BE} for a small transistor before and after irradiation.

To best fit the data, one radiation-induced trap was added to the small device after irradiation, two were added to the medium one, and five were added to the large one (B=$5.2\times10^{-18}A-cm$), consistent with a uniform trap generation rate at the device perimeter. The post-radiation calculation results are shown in Fig. 9, and are in agreement with the measured data. The calculated results of average post-radiation noise magnitude are also close to the data, but for brevity are not shown.

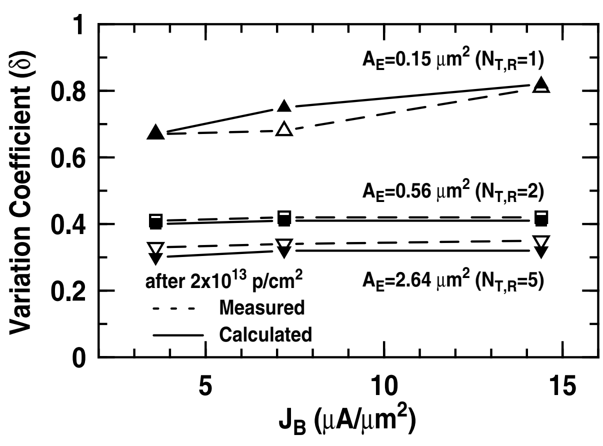

Fig. 9. Noise variation from measured and calculated noise spectra versus J_B after irradiation. The number of additional traps used in calculations is indicated for each size.

As shown in Fig. 8, the radiation-induced non-ideal base leakage current is relatively large and clearly not caused by only the few extra radiation-induced traps quantified in the noise calculations alone. Hence, the noise level of the majority of the radiation induced traps must be significantly lower than the pre-radiation noise level, and are thus effectively "hidden" in the overall spectra and are not observable.

V. Summary

We have investigated for the first time effects of proton irradiation on the low-frequency noise variation in aggressively-scaled SiGe HBTs. The pre-radiation LFN variation is geometry dependent and largest for the smallest devices, but shows little dependence on bias. After radiation, however, the overall noise magnitude shows little degradation, but the noise variation decreases significantly for the small devices, and shows both geometry and bias dependence.

The pre-radiation noise can be expressed as a superposition of individual G/R traps, and the number of G/R trap centers is proportional to the area of the transistors. The calculation shows a small number of pre-radiation traps leads to a large noise variation. The radiation-induced noise is written as another set of superposed G/R traps and added to the pre-radiation expression. The number of induced G/R traps is proportional to the emitter perimeter. Calculations show that such radiation-induced traps can decrease the noise variation, consistent with the data.

Advanced device technologies with aggressively-scaled emitter geometries have a size-dependent low-frequency noise variation, and this variation is sensitive to proton irradiation. This size variation is believed to be fundamental to scaled bipolar technologies, and thus is of potential concern for noise-sensitive circuits operating in the radiation environment.

Acknowledgment

The wafers were fabricated at IBM Microelectronics, Essex Junction, VT. The authors would like to thank G. Niu, Y. Li, X. Liu, L. Cohn, B. Kauffman, D. Harame, D. Ahlgren, G. Freeman, B. Meyerson, D. Herman, and the IBM SiGe team for their contributions to this work.

References

[1] M. Sanden *et al*., IEEE Trans. Electron Devices, vol. 49, pp. 514-520, 2002.
[2] Z. Jin *et al*., Proc. of the 2002 BCTM, pp. 224-227, 2002.
[3] A.L. McWhorter, Lincoln Laboratory Report, no. 80, Boston, May 1955.
[4] M.J. Uren *et al*., Appl. Phys. Lett., vol. 47, pp. 1195-1197, 1985.
[5] K. Kandiah, IEEE Trans. Electron Devices, vol. 41, pp. 2006-2015, 1994.
[6] L.S. Vempati *et al*., IEEE J. Solid-State Circuits, vol. 31, pp. 1458-1467, 1996.
[7] P. Llinares *et al*., J. Applied Physics, 82(5), pp. 2671-2675, 1997.
[8] W.S. Lau *et al*., Japan J. Applied Physics: Part 2 Letter, vol. 31. no. 8A, pp. L1021-L1023 ,1992.
[9] M.J. Deen *et al*., J. Applied Physics, 84(1), pp. 625-633, 1998.
[10] R. Plana *et al*., IEEE Electron Device Letters, vol. 16, pp. 58 -60, 1995.
[11] H.A.W. Markus *et al*., IEEE Trans. Electron Devices, vol. 42, pp. 720-727, 1995.
[12] A. Mounib *et al*., IEEE Trans. Electron Devices, vol. 42, pp. 1647-1652, 1995.
[13] F.N. Hooge, IEEE Trans. Electron Devices, vol. 41, pp. 1926-1935, 1994.
[14] J. Kilmer *et al*., Solid State Electronics, vol. 26, no. 1, pp. 71-74, 1983.
[15] L.K.J. Vandamme *et al*., IEEE Trans. Electron Devices, vol. 41, no. 11, pp. 1936-1945, 1994.
[16] T.G.M. Kleinpenning, Physica B & C, vol. 98, no. 4, pp. 289-299, 1980.
[17] L.K.J. Vandamme *et al*., Solid State Electronics, vol. 41, pp. 901-908, 1997.
[18] A. Joseph *et al*., Proceedings of the 2001 BCTM, pp.143-146, 2001.
[19] Z. Jin *et al*., IEEE Trans. Nuclear Science, vol. 48, pp. 2244-2249, 2001.
[20] K.M. Murray *et al*., Nucl. Inst. Meth., vol. B56/57, p. 616, 1991.
[21] P.W. Marshall *et al*., IEEE Trans. Nuclear Science, vol. 41, pp. 1958-1965, 1994.